Biogeosciences Discuss., https://doi.org/10.5194/bg-2018-446
Manuscript under review for journal Biogeosciences
Discussion started: 1 November 2018

Nitric oxide (NO) in the Bohai and Yellow Seas

Ye Tian[1,3], Chao Xue[1,3], Chun-Ying Liu[1,3,*] , Gui-Peng Yang[1,2,**], Pei-Feng Li[1,3], Wei-Hua Feng[4], and Hermann W. Bange[5]

[1]Key Laboratory of Marine Chemistry Theory and Technology, Ministry of Education, Qingdao, 266100, China
[2]Laboratory for Marine Ecology and Environmental Science, Qingdao National Laboratory for Marine Science and Technology, Qingdao 266071, China
[3]College of Chemistry and Chemical Engineering, Ocean University of China, Qingdao, 266100, China
[4]Key Laboratory of Engineering Oceanography, Second Institute of Oceanography, SOA, Hangzhou, 310012, China
[5]GEOMAR Helmholtz-Zentrum für Ozeanforschung Kiel, Kiel, 24105, Germany

Correspondence to: *Chun-Ying Liu (roseliu@ouc.edu.cn); **Gui-Peng Yang (gpyang@ouc.edu.cn)

Abstract. Nitric oxide (NO) is a short-lived compound of the marine nitrogen cycle; however, our knowledge about its oceanic distribution and pathways is rudimentary. Here we present the measurements of dissolved NO in the surface and bottom layers at 75 stations in the Bohai Sea (BS) and Yellow Sea (YS) in June 2011. Moreover, NO photoproduction rates were determined at 27 stations in both seas. The NO concentrations in the surface and bottom layers were highly variable and ranged from below the detection limit (i.e. 32 pmol L^{-1}) to 616 pmol L^{-1} in the surface layer and to 482 pmol L^{-1} in the bottom layer. There was no significant difference between the mean NO concentrations in the surface (186 ± 108 pmol L^{-1}) and bottom (174 ± 123 pmol L^{-1}) layers. A decreasing trend of NO bottom layer concentrations salinity indicates a NO input by submarine groundwater discharge. NO in the surface layer was supersaturated at all stations during both day and night and therefore the BS and YS were a persistent source of NO to the atmosphere at the time of our measurements. The accumulation of NO during daytime was resulting from photochemical production and photoprodcution rates were correlated to illuminance. The persistent nighttime NO supersaturation pointed to a, so far unknown, NO dark production. NO sea-to-air flux densities were much lower than the NO photoproduction rates. Therefore, we conclude that the bulk of the NO produced in the mixed layer was rapidly consumed before its release to the atmosphere. Overall, the oceanic NO emissions to the atmosphere were negligible compared to anthropogenic NO_x sources such as emissions from ships.

Introduction

Nitric oxide (NO) is a short-lived intermediate of the oceanic nitrogen cycle (Bange, 2008). It received limited attention so far because its determination in seawater is challenging (Zafiriou and McFarland, 1980; Lutterbeck and Bange, 2015; Liu et al., 2017). NO in surface seawater can be produced via the photolysis of nitrite (NO_2^-) (Zafiriou and McFarland, 1981; Olasehinde et al., 2009; 2010; Liu et al., 2017):

$$NO_2^- + H_2O \xrightarrow{h\nu} NO + OH^-.$$

This reaction may account for 10 % of nitrite loss in surface waters of the central equatorial Pacific (Zafiriou et al., 1980). Zafiriou and McFarland (1981) suggested that photochemically produced NO is a potential source of atmospheric NO during daylight. Apart from the photochemical production, various microbial pathways of NO have been identified including denitrification, nitrification and anammox (Schreiber et al., 2014; Martens-Habbena et al., 2015; Caranto and Lancaster, 2017; Kuypers et al., 2018). Additionally, NO is a messenger molecule in marine organisms: phytoplankton does not only response to exogenous NO (Zhang et al., 2005), but also produce NO during their growth (Zhang et al., 2006a, b; Kim et al., 2006, 2008). Chen et al. (2015) reported that calmodulin (a messenger protein expressed in eukaryotic cells) of the tropical sea cucumber participates in the production of NO during immune response. Morrall et al. (1998; 2000) characterized the NO synthase activity in the tropical sea anemone *Aiptasia pallida*, suggesting that NO and NO synthase can act as ecotoxicological biomarkers in the tropical marine environment. Moreover, the characterization of NO synthase gene in the intertidal copepod *Tigriopus japonicas* has been found and the intracellular production of NO in shrimp haemocytes has been observed (Xian et al., 2013; Jeong et al., 2016). Thus, NO seems to be widespread with different functions in marine organisms.

Current understanding of the oceanic NO distribution is mainly limited to the ocean surface (Zafiriou and McFarland, 1981; Olasehinde at al., 2009; 2010; Liu et al., 2017) and oxygen minimum zones (Ward and Zafiriou, 1988; Lutterbeck et al., 2018). Only recently, the distribution of NO as well as its seasonal variation in the Jiaozhou Bay and adjacent waters were studied (Feng et al., 2011; Xue et al., 2012; Tian et al., 2016).

In this study, we present first measurements of dissolved NO in the Yellow Sea (YS) and the Bohai Sea (BS). The overarching objective of our study was to decipher the biogeochemical fluxes of NO in the BS and YS. The specific objectives were (i) to determine the spatial variation of dissolved NO concentrations in the water column, (ii) to determine NO photoproduction rates, and (iii) to estimate the sea-to-air gas exchange fluxes of NO.

2 Materials and methods

2.1 Study area

The BS and the YS are marginal seas of the western Pacific Ocean. The BS is a shallow and almost enclosed sea with a surface area of 77×10^3 km^2 and a volume of 1.39×10^3 km^3. Its maximum depth is 83 m with an average depth of only 18 m. The Huanghe River is a major source of freshwater to the BS whereas the YS is the source of salt for the BS through water exchange via the Bohai Strait. The YS has a surface area of 380×10^3 km^2 and total volume of 16.7×10^3 km^3. Maximum depth is 140 m with an average depth of 44 m, and like the BS, it is a continental shelf sea. The Yangtze River at the southwest corner of the YS is the major source of freshwater for the southern YS and the East China Sea. The hydrographic properties of this region are mainly influenced by the Yellow Sea Cold Water Mass (YSCWM) on the shelf (Lü et al., 2010; Li et al., 2016) and the Yellow Sea Coastal Currents on the western side of the basin (Su, 1998; Lee et al., 2002; Zhang et al.,

2004). The BS and YS are regions surrounded by areas of high population growth and economic development in China and Korea (Zhan et al., 2010; Jiang et al., 2014).

2.2 Sampling

Samples were collected from 13 to 28 June 2011 on board of the R/V "Dong Fang Hong 2" in the BS and the YS. Sampling for NO from both the surface (at 1 m) and the bottom layer (= 1 m above the ocean bottom) were performed at 75 sampling stations (including one 24 h anchor station: B65) shown in Fig. 1 and listed in Table 1. Water samples were collected using 8-liter Niskin bottles equipped with silicon O-rings and Teflon-coated springs and mounted on a Sea-Bird CTD (conductivity, temperature, depth) instrument (Sea-Bird Electronics, Inc., USA). A 500 mL Wheaton glass serum bottle was rinsed with in situ seawater three times, and then was filled with seawater quickly through a siphon. When the overflowed sample reached the half volume of the bottle, the siphon was withdrawn rapidly, 0.5 mL saturated $HgCl_2$ (aq) solution was added, and the bottle was sealed quickly. The surface water samples were immediately analyzed after collection, and samples from other depths were temporarily placed in dark in a water bath with a surface seawater circulation system and analyzed within 1 hour (Liu et al., 2017). Photoproduction rates were determined in surface water samples from 22 stations in the YS (H01, H05, H08, H10, H17, H21, H25, H29, H31, H35, H37, H39, H42 B01, B05, B10, B12, B15, B18, B23, B27, and B35) and 4 stations in the BS (B42, B47, B51, and B68), respectively.

2.3 Analytical procedures

Analysis for dissolved NO was conducted with the improved method of Liu et al. (2017) by a combined purge-and-trap and fluorometric detection method. The precision of the analytical method was better than ± 7 % and the limit of detection (LOD) was 32 pmol L^{-1} (Liu et al., 2017).

The photolysis experiments were conducted under natural light conditions on deck. Surface water samples were filtered with 0.45 μm Millipore membrane and transferred into 10 mL cleaned quartz vials wrapped with Al foil with no headspace. Then 200 μL NaN_3 solutions were added. After the addition of 10 μL 1×10^{-3} mol L^{-1} 2, 3-diaminonaphthalene solution and gentle mixing, the fluorescence of the mixed solution was measured before irradiation (Liu et al., 2017). Then capped with a Teflon-lined silicone septum and without Al foil, the vial was placed in a shallow circulating seawater bath. The fluorescence of the solution was analyzed after irradiation for 0.5 hour. For dark controls, vials were wrapped in Al-foil. The quartz vials and syringe used in the experiment were soaked in a 10 % (v/v) HCl bath for 24 h, rinsed with Milli-Q water and baked at 500 ℃ for 4 hours.

Chlorophyll *a* (Chl-*a*) was fluorometrically measured by an F-4500 fluorescence spectrophotometer after filtration of 200 mL seawater through a Whatman glass fiber filter and extraction in 90 % acetone according to Strickland and Parsons (1968). The wind speeds were measured at a height of 10 m above the sea surface using a Model 27600-4X ship-borne weather instrument (Young, USA). Illuminance was measured by a digital illuminometer (TES-1330A, Shenzhen, China). Dissolved oxygen (DO) was measured in discrete water samples by the Winkler method (Grasshoff et al., 2009). The concentrations of

dissolved inorganic nitrogen (nitrate, nitrite, and ammonium) were analyzed using a nutrient automatic analyzer (Auto Analyzer 3, SEAL Analytical, USA) in the laboratory. The detection limits were 0.14 μmol L^{-1} for nitrate, nitrite, and ammonium, with the precision of the method exceeding 3 % (Liu et al., 2005).

2.4 Calculation of NO flux and NO saturation

Fluxes of NO across the sea-to-air interface were estimated following the approach of McGillis et al. (2000) for a sparingly soluble gas which is also moderately reactive in the atmosphere:

$F = k_{sea} (c_{sea} - p\mathrm{NO}_{air} \times H^{cp})$,

here F stands for the flux density (mass $area^{-1}$ $time^{-1}$) across the air-sea interface, k_{sea} is the gas transfer velocity (length $time^{-1}$), and c_{sea} is the measured concentration of NO in the surface seawater (mass $volumn^{-1}$). The partial pressure of the atmospheric NO ($p\mathrm{NO}_{air}$) was calculated as:

$p\mathrm{NO}_{air} = x'\mathrm{NO}_{air} \times (p_{ss} - p_w)$,

where $x'\mathrm{NO}_{air}$ is the mole fraction of atmosphere NO (dimensionless). We used the value of 2.13 ppb for $x'\mathrm{NO}_{air}$ which is the average atmospheric NO mole fraction over the YS (Hu Min, Peking University, personal communication, 2018). And p_{ss} is the barometric pressure at sea surface which was set to 1 atm as the average pressure and p_w is the water vapor pressure at sea surface which was calculated after Weiss and Price (1980):

$\ln p_w = 24.4543 - 6745.09 / (T + 273.15) - 4.8489 \times \ln (T + 273.15) / 100) - 0.000544 \times S)$.

H^{cp} is the Henry's law constant which is calculated as:

$H^{cp}(\mathrm{T}) = H^{\Theta} \times \exp (- \Delta\mathrm{sol}\, H / R \times (1 / T - 1 / T^{\Theta})$

where $-\Delta sol \frac{H}{R} = \frac{dlnH}{dln(\frac{1}{T})}$.

H^{Θ}, and $-\Delta\mathrm{sol}\, H / R$ are tabulated in Sander (2015).

k_{sea} was calculated as:

$k_{sea} = k_w (1 - \gamma_a)$,

$\gamma_a = 1 / (1 + (k_a / (H^{cc} \times k_w))$,

$H^{cc} = H^{cp} \times RT$,

$k_a = 659 \times u \times (\mathrm{M_{NO}} / \mathrm{M_{H_2O}})^{-1/2}$,

$k_w = 0.251 \times u^2 \times (\mathrm{Sc} / 660)^{-1/2}$,

where k_w is the water side air-sea gas transfer coefficient for sparingly soluble gases (length $time^{-1}$) calculated according to Wanninkhof (2014), γ_a is the fraction of the entire gas concentration gradient across the airside boundary layer as a fraction of the entire gradient from the bulk water to the bulk air (dimensionless) (McGillis et al., 2000), k_a is the air side air-sea gas transfer coefficient (length $time^{-1}$) according to McGillis et al. (2000), H^{cc} is the Henry coefficient (dimensionless) (Sander, 2015), $\mathrm{M_{NO}}$ and $\mathrm{M_{H_2O}}$ are relative molecular mass of NO and H_2O (dimensionless), and u is the wind speed at 10 m height under neutral boundary conditions (length $time^{-1}$).

The Schmidt number (Sc) is the kinematic viscosity of water divided by the molecular diffusion coefficient of the gas in (sea)water (Jähne et al., 1987; Wanninkhof, 2014). Seawater dynamic viscosity (μ_{sw}) is a function of temperature (T) and salinity (S) and was estimated using the following equations (Sharqawy et al., 2010):

$$\mu_{sw} = \mu_w (1 + A S + B S^2),$$

$$A = 1.541 + 1.998\times10^{-2} T - 9.52\times10^{-5} T^2,$$

$$B = 7.974 - 7.561\times10^{-2} T + 4.724\times10^{-4} T^2,$$

$$\mu_w = 4.2844\times10^{-5} + (0.157 (T + 64.993)^2 - 91.296)^{-1}.$$

Seawater density was estimated using Millero's empirical equation (Millero et al., 1976), and NO diffusion coefficient in water was calculated according to Wise and Houghton (1968):

$$D_L = 0.9419 \exp(0.0447 T).$$

The saturation factor (α) is defined as $\alpha = c_{sea} / (p\mathrm{NO}_{air}\times H^{cp})$, $\alpha > 1$ represents NO was supersaturated and the flux was from sea to air.

3 Results and Discussion

3.1 NO in the surface and bottom layers

The NO concentrations from the surface and bottom layers of the BS and the YS as well as the local sampling time, bottom depth (D), temperature (T), salinity (S), Chl-*a*, wind speed (u), and DO are listed in Table 1. The surface concentrations of NO ranged from below the LOD to 616 pmol L^{-1} with an overall average of 186 ± 108 pmol L^{-1} and exhibited a considerable spatial variability (Fig. 2a). The mean NO surface concentrations in the BS (203 ± 107) and northern YS (NYS) (212 ± 130) were higher than the mean NO concentration in the southern YS (SYS) (159 ± 84). The NO concentrations in the bottom layer ranged from below the LOD to 482 pmol L^{-1}, with an overall average of 174 ± 123 pmol L^{-1}. The mean concentrations of NO in the bottom layers of the BS and NYS were 228 ± 116, 210 ± 138, respectively and were higher than the mean (127 ± 98 pmol L^{-1}) for the SYS. The maximum NO surface and bottom concentrations were measured at stations B21 and B28 in the NYS, respectively (Fig. 2b), whereas the lowest NO surface and bottom concentrations were measured in the center of the SYS (Table 1). Overall, there were no statistically significant differences between the mean NO concentrations in the surface and bottom layers.

NO surface concentrations did not show any statistically significant relationship with depth, sea surface temperature, salinity, DO, Chl-*a*, and illuminance. Trends of NO concentrations with salinity and DIN were was only found for the stations affected by the outflow of the Huanghe River in the southern BS (Fig. 3) where we found an inverse relationship between salinity and NO surface concentrations. High NO concentrations were associated with high DIN concentrations (data not shown, see Liu et al., 2015; Yang et al, 2015) indicating that DIN, especially NO_2^-, was a prerequisite for enhanced NO concentrations.

The water columns of the BS and YS were well-oxygenated during our study and, thus, no suboxic or anoxic conditions were detected. Therefore, we did not found any enhancement of NO concentrations in the bottom layers with low DO or NO_2^- concentrations as observed in the OMZ of the eastern tropical South Pacific Ocean off Peru (Lutterbeck et al., 2018). However, NO concentrations in the bottom layer showed negative correlations with salinity ($p < 0.05$, $R = -0.258$) and bottom depth ($p < 0.05$, $R = -0.292$) indicating a decrease of NO concentrations from the coast toward offshore waters. It is known that both the BS and YS are affected by submarine ground water discharge (Kim et al., 2005; Liu et al., 2017a; 2017b; Taniguchi et al. 2008). Moreover, NO has been detected in groundwater and aquifers (Smith et al., 2004, Smith and Yoshinari, 2008). Therefore, we suggest that input of NO from submarine groundwater discharge contributed to the distribution of NO bottom concentrations as well.

An overview of published NO surface concentrations is given Table 3. The average NO surface and bottom concentrations from this study are comparable to the concentrations measured in the Jiaozhou Bay, in the waters off Qingdao and in the Seto Inland Sea. However, our mean concentrations are considerably higher than the NO concentrations reported from the central equatorial Pacific and then eastern tropical North Pacific Ocean. The maximum concentration reported here is at the lower end of the NO concentrations recently reported from the anoxic oxygen minimum zone off Peru. Overall, NO surface concentrations NO seem to be generally higher in coastal waters compared to those found in offshore waters.

3.2 Diurnal variability

The diurnal variability of surface NO concentrations, illuminance, DO, and Chl-*a* were investigated at the anchor station B65 (Fig. 4). NO concentrations varied from 64 to 424 pmol L^{-1}, exhibiting a significant diurnal variation with the maximum concentration eightfold higher than the minimum concentration. The NO concentrations reached the maximum concentration in the early afternoon (about 13:00 local time, LT) and then decreased to the minimum concentration at 22:00 LT. A less pronounced second maximum (209 pmol L^{-1}) was reached at 04:00 LT. DO showed a similar diurnal cycle but shifted by three hours with maxima at 16:00 LT and 07:00 LT. Chl-*a* concentrations peaked at 19:00 LT and 07:00 LT. The illuminance had its maximum at 13:00 LT coinciding with the NO maximum indicating that the first NO maximum was indeed resulting from a photochemical production during daytime (Zafiriou and McFarland, 1981). However, the second maximum of NO at 04:00h, when it was still dark, must have resulted from an alternative chemical and/or biological production.

3.3 Photoproduction rates

The results of the NO photoproduction experiments are listed in Table 2. The photoproduction rates of NO in the BS, the NYS, and the SYS varied from 0.00 to 5.07×10^{-11} mol L^{-1} s^{-1}, 0.09 to 0.69×10^{-11} mol L^{-1} s^{-1}, and 0.32 to 1.54×10^{-11} mol L^{-1} s^{-1}, respectively. The average photoproduction rate of the whole study area was $1.14 \pm 1.37 \times 10^{-11}$ mol L^{-1} s^{-1}. The photoproduction rates from the BS and YS are in good agreement with the rates reported from Seto Inland Sea (Olasehinde et al, 2009; 2010). However, the mean NO photoproduction rates are higher than those from the central equatorial Pacific

Ocean (Zafiriou and McFarland, 1981) and lower than those from Kurose River, Japan (Olasehinde et al, 2009) (Table 2) which mirrors the available NO_2^- concentrations which are low in the open ocean and but high in a river.

The average photoproduction rate in the NYS was obviously lower than those in the BS and the SYS, consistent with the average illuminances, which were 22450, 20433, and 27825 lx for the BS, the NSY and the SYS, respectively. Enhanced photoproduction rates ($\geq 2.00 \times 10^{-11}$ mol L^{-1} s^{-1}) occurred in the SYS, especially in the central part of the southern SYS and stations influenced by the Yellow Sea Cold Current (see Fig. 1). This is apparently in contrast to the distribution of NO which showed lowest concentrations in the central SYS (see above). The high illumination observed in the SYS (Table 2) does not only lead to enhanced NO photoproduction (see Table 2) but also generate reactive oxygen species like O_2•-, ROO•, and other OH-derived radicals, which in turn can efficiently scavenge NO (Olasehinde et al, 2010). Overall, the NO photoproduction rates showed a positive relationship with illuminance ($p < 0.01$, $R = 0.884$) indicating that the NO concentrations in the surface layer during daylight was dominated by photochemical production. However, we did not find a significant difference between the mean NO concentrations sampled during day (179 ± 80 pmol L^{-1}) and night (195 ± 140 pmol L^{-1}). This suggests that there was also a non-photochemical NO dark production in the surface layer.

3.4 Sea-to-air fluxes of NO

In the present study, the NO supersaturation was ubiquitous at all investigated sites. The supersaturation factors varied from 8 to 154, with an average of 47. Together with the fact that that NO was supersaturated during daytime and nighttime during the 24h station B65 this indicates that the BS and YS were a source of NO to the atmosphere. The sea-to-air flux densities ranged from 5.8×10^{-19} to 3.6×10^{-15} mol cm^{-2} s^{-1}, with an average value of 4.5×10^{-16} mol cm^{-2} s^{-1} (Fig. 7). The comparison of wind speeds and flux densities reveal that the flux densities are mainly driven by the wind speed (Fig. 7) Our flux densities from the BS and YS were similar to those computed for the central equatorial Pacific Ocean and the Seto Inland Sea, while they are slightly lower than those computed for of Jiaozhou Bay waters (Table 2). Based on the YS area of 380×10^3 km^2 and the BS area of 77×10^3 km^2, the emission of NO to the atmosphere was estimated to be 9.0×10^8 g N yr^{-1} or 7.6×10^7 g N $month^{-1}$. Ding et al. (2018) report an satellite-derived average NO_x emission estimate for June over the BS and the YS in the period from 2007 to 2016 of about 1.3×10^{10} g N $month^{-1}$. The obvious very large discrepancy between the satellite-derived emission estimate and the one presented here results from the fact that Ding et al.'s (2018) estimate is dominated by the NO_x emissions from ships' diesel engines. This indicates that oceanic NO emissions to the atmosphere only account for a negligible fraction (~0.6 %) of the NO_x emissions observed over the BS and YS.

3.5 NO mixed layer budget

In order to estimate the contribution of different source and sinks of NO in surface layer of the BS and YS we applied a simple box model. We assume that the surface layer is represented by the mixed layer with a mean water depth of 15 m depth (Qiao et al., 2004). At steady state the loss of NO by air-sea exchange (F_{ase}) must be equal to the sum of the photoproduction rate (F_{pp}) in the mixed layer and the input from below into the mixed layer by diapycnal diffusion (F_{dia}) and

other production or consumption pathways (F_{poc}) and advection into or out of the BS/YS mixed layer (F_{adv}). To this end, F_{ase} is given by

$F_{ase} = F_{pp} + F_{dia} + F_{poc} + F_{adv}$.

The mean F_{ase} was 4.5×10^{-16} mol cm^{-2} s^{-1} (see above). We assume that the NO photoproduction decreases linearly from the average rate of $1.15 \pm 1.47 \times 10^{-11}$ mol L^{-1} s^{-1} at the surface (see above) to 0 at 15 m. The mean F_{pp} was calculated to be 8.6×10^{-12} mol cm^{-2} s^{-1} in mixed layer. Since the mean surface NO concentration in the surface layer was statistically not different from the mean NO concentration in the bottom layer (see above) it is reasonable to assume that $F_{dia} = 0$. Moreover, it seems reasonable to assume that advection of NO into or out of the BS/YS surface layer is zero. Since $F_{ase} < F_{pp}$ we conclude that F_{poc} should be negative indicating that the bulk of the produced NO was rapidly consumed in the surface layer before its release to the atmosphere. Please note that we have some indications that there is also a dark production of NO (see above), so that the 'true' NO surface production might be even higher. Chemical reactions with DO, OH, or ROO• etc. are potential sinks for NO in the surface layer of the BS and YS (Ford et al., 1993; Olasehinde et al, 2010; Carpenter and Nightingale, 2015).

4. Conclusions

This study reports the distribution and photoproduction rates of dissolved NO measured during a cruise in June 2011 to the Bohai and Yellow Seas. The NO concentrations in both the surface and bottom layers were highly variable. There was no significant difference between the mean NO concentrations in the surface and bottom layers. NO concentrations in the bottom layer showed significant decreasing with salinity indicates NO input by submarine groundwater disharge. NO in the surface layer was supersaturated at all stations during day and night. The accumulation of NO during daytime was resulting from photoproduction and the measured NO photoproduction rates were correlated to illuminance. The persistent nighttime NO supersaturation pointed to a, so far unknown, non-photochemical (chemical and/or biological) NO dark production. On the basis of a simple box model calculation we conclude that the bulk of the NO produced in the surface layer was rapidly consumed before its release to the atmosphere. Overall, the BS and YS were a persistent source of NO to the atmosphere at the time of our measurements. However, the oceanic NO emissions were negligible compared to the NO_x emissions from ships diesel engines.

Author contribution: Chun-Ying Liu and Gui-Peng Yang designed the experiments and Ye Tian, Chao Xue, Pei-Feng Li, and Wei-Hua Feng carried them out. Hermann W. Bange and Chun-Ying Liu analyzed the data and Ye Tian prepared the manuscript with contributions from all co-authors.

Competing interests. The authors declare that they have no conflict of interest.

Acknowledgements

We thank the captain and crew of the R/V "Dong Fang Hong 2" for their support and help during the cruise. This research was supported by the National Natural Science Foundation of China (Nos.41676065 and 40706040), the National Key Research and Development Program of China (Grant No. 2016YFA0601301), the Fundamental Research Funds for the Central Universities (No. 201762032), and the AoShan Talents Program of Qingdao

References

Bange, H.W.: Chapter 2 - Gaseous Nitrogen Compounds (NO, N_2O, N_2, NH_3) in the Ocean. Nitrogen in the Marine Environment (Second Edition), Elsevier, Amsterdam, Netherlands, 51-94, 2008.

Caranto, J.D. and Lancaster, K.M.: Nitric oxide is an obligate bacterial nitrification intermediate produced by hydroxylamine oxidoreductase, PNAS., 114, 8217, https://doi.org/10.1073/pnas.1704504114, 2017.

Carpenter, L.J. and Nightingale, P.D.: Chemistry and Release of Gases from the Surface Ocean. Chemical Reviews, Chem. Rev., 115(10), 4015-4034, https://doi.org/10.1021/cr5007123, 2015.

Chen, T., Ren, C., Li, W., Jiang, X., Xia, J., Wong, N.K., and Hu, C.: Calmodulin of the tropical sea cucumber: gene structure, inducible expression and contribution to nitric oxide production and pathogen clearance during immune response, Fish Shellfish Immunol., 45(2), 45(2), 231-238. https://doi.org/10.1016/j.fsi.2015.04.013, 231-238, 2015.

Dang, H., Zhou, H., Zhang, Z., Yu, Z., Hua, E., Liu, X., and Jiao, N.Z.: Molecular detection of *Candidatus Scalindua* pacifica and environmental responses of sediment anammox bacterial community in the Bohai Sea, China, Plos One, 8, e61330, https://doi.org/10.1371/journal.pone.0061330, 2013.

Ding, J. R., Ronald, V.D.A., Mijling, B., Jalkanen, J.P., Johansson, L. and Levelt, P.F.: Maritime NOx emissions over Chinese seas derived from satellite observations, Geophys. Res. Lett., 45(9), https://doi.org/10.1002/2017gl076788, 2018.

Feng, W.H., Liu, C.Y., Yang, G.P., Li, P.F., and Xue, C.: Chemiluminescene detection of nitric oxide in seawater, Acta Oceanol. Sin., 33 (6), 93-98, 2011. (In Chinese with English abstract)

Ford, P.C., Wink, D.A., Stanbury, D.M.: Autoxidation kinetics of aqueous nitric oxide, Febs Lett., 326(1-3):1, https://doi.org/10.1016/0014-5793(93)81748-o, 1993,

Grasshoff, K., Kremling, K., and Ehrhardt, M.: Methods of seawater analysis, John Wiley & Sons, New York, American, 2009.

Jeong, C.B., Kang, H.M., Seo, J.S., Park, H.G., Rhee, J.S., and Lee, J.S.: Identification and molecular characterization of nitric oxide synthase (NOS) gene in the intertidal copepod Tigriopus japonicas, Gene, 577(1), 47, https://doi.org/10.1016/j.gene.2015.11.019, 2016.

Jiang, X., Teng, A., Xu, W., and Liu, X.: Distribution and pollution assessment of heavy metals in surface sediments in the Yellow Sea, Mar. Pollut. Bull., 83 (1), 366-375, https://doi.org/10.1016/j.marpolbul.2014.03.020, 2014.

Jähne, B., Heinz, G., and Dietrich, W.: Measurement of the diffusion coefficients of sparingly soluble gases in water, J. Geophys. Res.: Oceans, 92(C10):10767-10776, https://doi.org/10.1029/jc092ic10p10767, 1987.

Kim, D., Yamaguchi, K., and Oda, T.: Nitric oxide synthase-like enzyme mediated nitric oxide generation by harmful red tide phytoplankton, J. Plankton Res., 28(6), 613-620, https://doi.org/10.1093/plankt/fbi145, 2006.

Kim, D., Yang, S.K., Lee, Y., Yamaguchi, K., Matsuoka, K., Lee, K.W., Choi, K.S., and Oda, T.: Detection of nitric oxide (NO) in marine phytoplankters, J. Biosci. Bioeng., 105 (4), 414-417, https://doi.org/10.1263/jbb.105.414, 2008.

Kim, G., Ryu, J. W., Yang, H. S., and Yun, S. T.: Submarine groundwater discharge (SGD) into the Yellow Sea revealed by 228 Ra and 226 Ra isotopes: Implications for global silicate fluxes, Earth Planet, Sci. Lett., 237 (1-2), 156-166, https://doi.org/10.1016/j.epsl.2005.06.011, 2005.

Kuypers, M.M.M., Marchant, H.K., and Kartal, B.: The microbial nitrogen-cycling network, Nat. Rev. Microbiol., 16 (5), 263-276, https://doi.org/10.1038/nrmicro.2018.9, 2018.

Lee, H.J., Jung, K.T., So, J.K., and Chung, J.Y.: A three-dimensional mixed finite-difference Galerkin function model for the oceanic circulation in the Yellow Sea and the East China Sea in the presence of M_2 tide, Cont. Shelf Res., 22 (1), 67-91, https://doi.org/10.1016/s0278-4343(01)00068-1, 2002.

Li, J., Li, G., Xu, J., Dong, P., Qiao, L., Liu, S., Sun, P., and Fan, Z.: Seasonal evolution of the Yellow Sea Cold Water Mass and its interactions with ambient hydrodynamic system, J. Geophys. Res., 121 (9), 6779-6792, https://doi.org/10.1002/2016jc012186, 2016.

Liu, C.Y., Feng, W.H., Tian, Y., Yang, G.P., Li, P.F., and Bange, H.W.: Determination of dissolved nitric oxide in coastal waters of the Yellow Sea off Qingdao, Ocean Sci., 13 (4), 1-31, 13(4), 1-31. https://doi.org/10.5194/os-2017-10, 2017.

Liu, J., Du, J., and Yi, L.: Ra Tracer-Based Study of Submarine Groundwater Discharge and Associated Nutrient Fluxes into the Bohai Sea, China: A Highly Human-Affected Marginal Sea, J. Geophys. Res., 122 (1), 139-152, 2017a.

Liu, J. A., Su, N., Wang, X., and Du, J.: Submarine groundwater discharge and associated nutrient fluxes into the Southern Yellow Sea: A case study for semi-enclosed and oligotrophic seas-implication for green tide bloom, J. Geophys. Res.: Oceans, 122 (11), 8646-8660, https://doi.org/10.1002/2017jc013095, 2017b.

Liu, S.M., Zhang, J., Chen, H.T., and Zhang, G.S.: Factors influencing nutrient dynamics in the eutrophic Jiaozhou Bay, North China, Prog. Oceanogr., 66 (1), 66-85, 2005.

Liu, S.M.: Response of nutrient transports to water-sediment regulation events in the Huanghe basin and its impact on the biogeochemistry of the Bohai, J Marine Syst., 141, 59-70, https://doi.org/10.1002/2016jc012282, 2015.

Lutterbeck, H.E. and Bange, H.W.: An improved method for the determination of dissolved nitric oxide (NO) in seawater samples, Ocean Sci., 11 (6), 959-981, https://doi.org/10.5194/osd-12-959-2015, 2015.

Lutterbeck, H.E., Arévalo-Martínez, D.L., Löscher, C.R., and Bange, H.W.: Nitric oxide (NO) in the oxygen minimum zone off Peru, Deep-Sea Res. Part II, in press, 2018.

Lü, X., Qiao, F., Xia, C., Wang, G., and Yuan, Y.: Upwelling and surface cold patches in the Yellow Sea in summer: Effects of tidal mixing on the vertical circulation, Cont. Shelf Res., 30 (6), 620-632, https://doi.org/10.1016/j.csr.2009.09.002, 2010.

Martens-Habbena, W., Qin, W., Horak, R.E., Urakawa, H., Schauer, A.J., Moffett, J.W., Armbrust, E.V., Ingalls, A.E., Devol, A.H., and Stahl, D.A.: The production of nitric oxide by marine ammonia-oxidizing archaea and inhibition of archaeal ammonia oxidation by a nitric oxide scavenger, Environ. Microbiol., 17(7), 2261-2274, https://doi.org/10.1111/1462-2920.12677, 2015.

Mcgillis, W.R., Dacey, J.W.H., Frew, N.M., Bock, E.J., and Nelson, R.K.: Water-air flux of dimethylsulfide, J. Geophys. Res., 105(C1), 1187–1193, 2000.

Millero, F.J., Gonzalez, A., and Ward, G.K.: Density of seawater solutions at one atmosphere as a function of temperature and salinity, J. Mar. Res., 34(1), 61-93, 1976.

Morrall, C.E., Trapido-Rosenthal, H.G., Knap, A.H., and Depledge, M.H.: Development of nitric oxide and nitric oxide synthase as ecotoxicological biomarkers in the tropical marine environment, Mar. Environ. Res., 46, 429-432, https://doi.org/10.1016/s0141-1136(97)00080-9, 1998.

Morrall, C.E. and Galloway, T.S., Trapidorosenthal, H.G., Depledge, M.H.: Characterisation of nitric oxide synthase activity in the tropical sea anemone Aiptasia pallida, Comp. Biochem. Physiol., Part B: Biochem. Mol. Biol., 125 (4), 483-491, https://doi.org/10.1016/s0305-0491(00)00157-7, 2000.

Olasehinde, E.F., Takeda, K., and Sakugawa, H.: Development of an Analytical Method for Nitric Oxide Radical Determination in Natural Waters, Anal. Chem., 81 (16), 6843-6850. https://doi.org/10.1021/ac901128y, 6843-6850, 2009.

Qiao, F.L., Xia C.S., Shi J.W.: Seasonal variability of thermocline in the Yellow Sea, Chin. J. Oceanol. Limnol., 22 (3):299-305, 2004.

Sander, R.: Compilation of Henry's law constants (version 4.0) for water as solvent, Atmos. Chem. Phys., 14 (21), 29615-30521, https://doi.org/10.5194/acp-15-4399-2015, 2015.

Schreiber, F., Stief, P., Kuypers, M.M.M., and De Beer, D.: Nitric oxide turnover in permeable river sediment, Limnol. Oceanogr., 59 (4), 1310-1320, https://doi.org/10.4319/lo.2014.59.4.1310, 2014.

Sharqawy, M. H., V, J. H. L., and Zubair, S. M.: Thermophysical properties of seawater: a review of existing correlations and data, Desalination & Water Treatment, 16 (1-3), 354-380, https://doi.org/10.5004/dwt.2010.1079, 2010.

Smith, R. L., Böhlke, J. K., Garabedian, S. P., Revesz, K. M., and Yoshinari, T.: Assessing denitrification in groundwater using natural gradient tracer tests with 15 N: In situ measurement of a sequential multistep reaction, Water Resources Res, 40 (7), 1-17, https://doi.org/10.1029/2003wr002919, 2004.

Smith, R. L., and Yoshinari, T.: Occurrence and turnover of nitric oxide in a nitrogen-impacted sand and gravel aquifer, Environ. Sci. Technol., 42 (22), 8245, https://doi.org/10.1021/es801290v, 2008.

Strickland, J.D.H. and Parsons T.R.: A practical handbook of seawater analysis. Fisheries Research Board of Canada, Ottowa, 1968.

Su, J.: Circulation dynamics of the China seas: north of 18 °N, The Sea., 6, 13-19, 1998.

Taniguchi, M., Ishitobi, T., Chen, J., Onodera, S. I., Miyaoka, K., Burnett, W. C., Peterson, R., Liu, G., and Fukushima, Y.: Submarine groundwater discharge from the Yellow River Delta to the Bohai Sea, China, J. Geophys. Res.: Oceans, 113, C06025, https://doi.org/10.1029/2007jc004498, 2008.

Tian, Y., Xue, C., Liu, C.Y., and Li, P.F.: Distribution and influencing factors of nitric oxide in the surface water of Jiaozhou Bay, Res. Environ. Sci., 29 (10), 1451-1458, 2016. (In Chinese with English abstract)

Wanninkhof, R.: Relationship between wind speed and gas exchange over the ocean revisited, Limnol. Oceanogr., 12, 351-362, https://doi.org/10.4319/lom.2014.12.351, 2014.

Ward, B.B. and Zafiriou, O.C.: Nitrification and nitric oxide in the oxygen minimum of the eastern tropical North Pacific, Deep-Sea Res., Part I, 35(7):1127-1142, https://doi.org/10.1016/0198-0149(88)90005-2, 1988.

Weiss, R.F. and. Price, B.A.: Nitrous oxide solubility in water and seawater, Mar. Chem., 8(4):347-359, https://doi.org/10.1016/0304-4203(80)90024-9, 1980.

Wise, D.L. and Houghton, G.: Diffusion coefficients of neon, krypton, xenon, carbon monoxide and nitric oxide in water at 10-60 ℃. Chem. Eng. Sci., 23, 1211-1216, https://doi.org/10.1016/0009-2509(68)89029-3, 1968.

Xian, J.A., Guo, H., Li, B., Miao, Y.T., Ye, J.M., Zhang, S.P., Pan, X.B., Ye, C.X., Wang, A.L., and Hao, X.M.: Measurement of intracellular nitric oxide (NO) production in shrimp haemocytes by flow cytometry, Fish Shellfish Immunol., 35, 2032-2039, https://doi.org/10.1016/j.fsi.2013.10.014, 2013.

Xue, C., Liu, C.Y., Yang G.P., Zhu, C.J., Chen, J., and Zhang, H.H.: Distribution and Controlling Factors of Nitric Oxide Concentrations in Surface Seawater of Jiaozhou Bay and Adjacent Waters, Chin. J. Environ. Sci., 33 (4), 1086-1090, 2012. (In Chinese with English abstract)

Yang, J., Yang G.P., Zhang, H.H., and Zhang, S.H.: Spatial distribution of dimethylsulfide and dimethyl-sulfoniopropionate in the Yellow Sea and Bohai Sea during summer, Chin. J. Oceanol. Limnol., 33 (4), 1020-1038, https://doi.org/10.1007/s00343-015-4188-5, 2015.

Zafiriou, O.C., Mcfarland, M., and Bromund, R.H.: Nitric oxide in seawater, Science, 207 (4431), 637-639, https://doi.org/10.1126/science.207.4431.637, 1980.

Zafiriou, O.C. and Mcfarland, M.: Nitric oxide from nitrite photolysis in the central equatorial Pacific, J. Geophys. Res.: Atmos., 86 (C4), 3173-3182, https://doi.org/10.1029/jc086ic04p03173, 1981.

Zhan, S., Peng, S., Liu, C., Chang, Q., and Jian, X.: Spatial and Temporal Variations of Heavy Metals in Surface Sediments in Bohai Bay, North China, Bull. Environ. Contam. Toxicol., 84 (4), 482-487, https://doi.org/10.1007/s00128-010-9971-6, 2010.

Zhang, J., Yu, Z.G., Raabe, T., Liu, S.M., Starke, A., Zou, L., Gao, H.W. and Brockmann, U.: Dynamics of inorganic nutrient species in the Bohai seawaters, J. Mar. Syst., 44 (3-4), 189-212, https://doi.org/10.1016/j.jmarsys.2003.09.010, 2004.

Zhang, Z.B., Lin, C., Liu, C., and Lei, X.: Study on patterns and chemical features of NO effect on marine phytoplankton growth. Sci. China: Chem., 48 (4), 376-384, https://doi.org/10.1360/03yb0166, 2005.

Zhang, Z.B., Xing, L., Wu, Z.Z., Liu, C.Y., Lin, C., and Liu, L.S.: Discovery of nitric oxide in marine ecological system and the chemical characteristics of nitric oxide. Sci. China: Chem., 49 (5), 475-480, https://doi.org/10.1007/s11426-006-2017-6, 2006a.

Zhang, Z.B., Liu, C.Y., Wu, Z.Z., Xing, L., and Li, P.F.: Detection of nitric oxide in culture media and studies on nitric oxide formation by marine microalgae, Med. Sci. Monit., 12, 75-85, 2006b.

Biogeosciences Discuss., https://doi.org/10.5194/bg-2018-446
Manuscript under review for journal Biogeosciences
Discussion started: 1 November 2018

Figure Captions

Figure 1. Locations of the sampling stations in the BS and the YS during summer.

Figure 2. Horizontal distributions of NO (pmol L^{-1}) in the surface water and bottom water.

Figure 3. Variations of salinity, NO surface concentrations, and NO_2^- concentrations from station B65 to station B70.

Figure 4. Diurnal variations of NO concentrations, illuminance (I), DO, and Chl-*a* concentrations in the surface water at the anchor station B65.

Figure 5. Wind speeds and flux densities of NO in the Bohai and Yellow Seas.

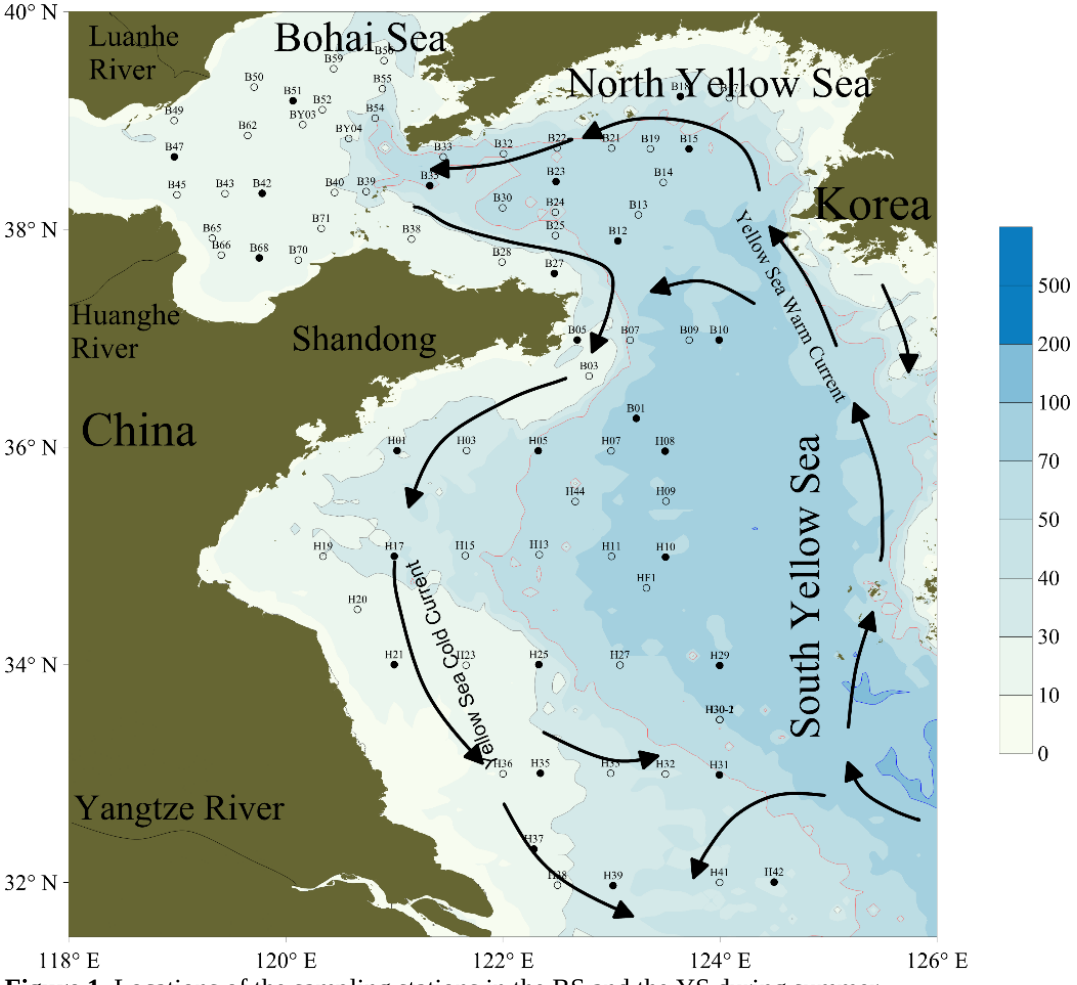

Figure 1. Locations of the sampling stations in the BS and the YS during summer. Solid dots (●) represent the stations for incubation experiments.

Biogeosciences Discuss., https://doi.org/10.5194/bg-2018-446
Manuscript under review for journal Biogeosciences
Discussion started: 1 November 2018

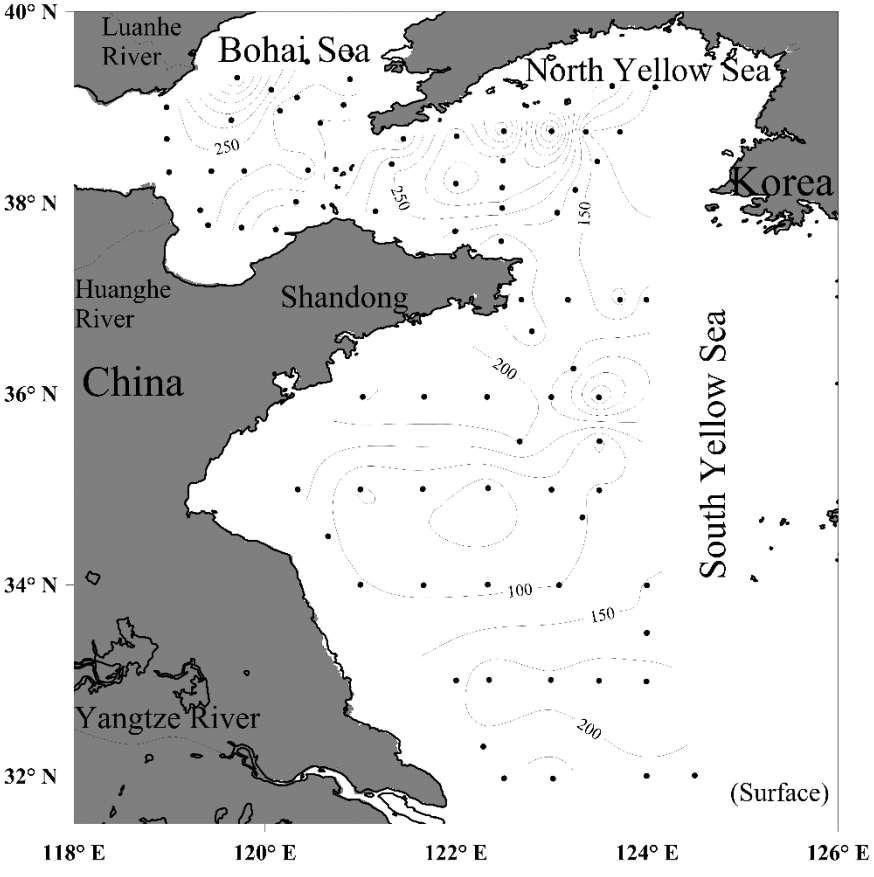

Biogeosciences Discuss., https://doi.org/10.5194/bg-2018-446
Manuscript under review for journal Biogeosciences
Discussion started: 1 November 2018

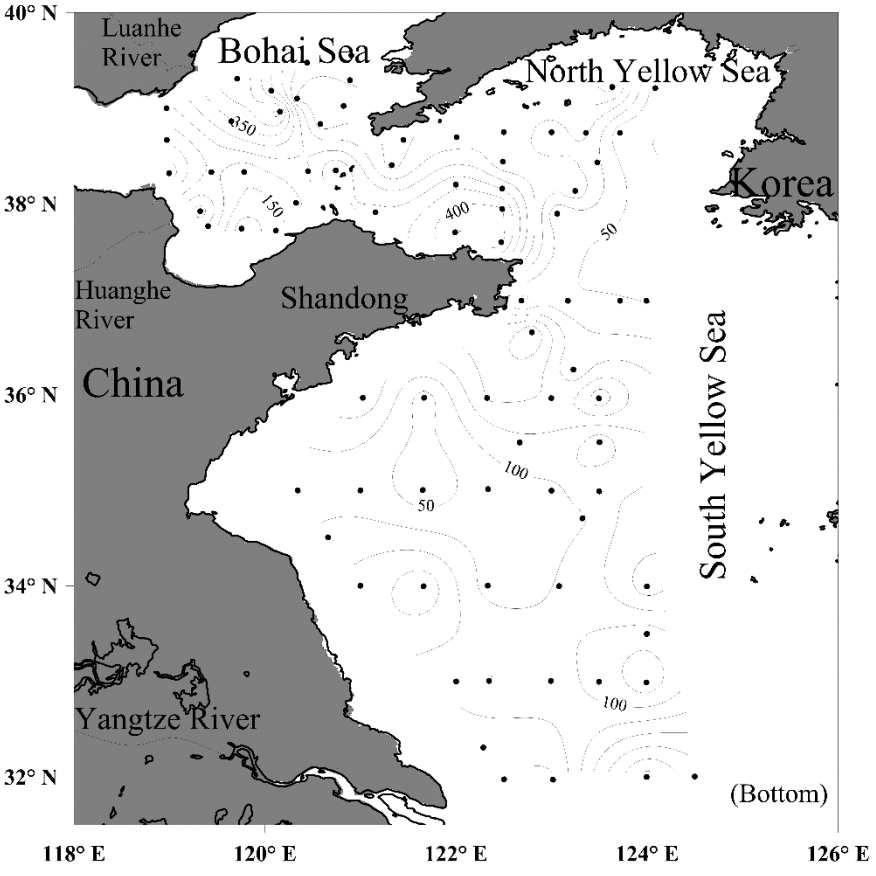

Figure 2. Horizontal distributions of NO (pmol Ł$^{-1}$) in the surface and bottom layers.

Biogeosciences Discuss., https://doi.org/10.5194/bg-2018-446
Manuscript under review for journal Biogeosciences
Discussion started: 1 November 2018

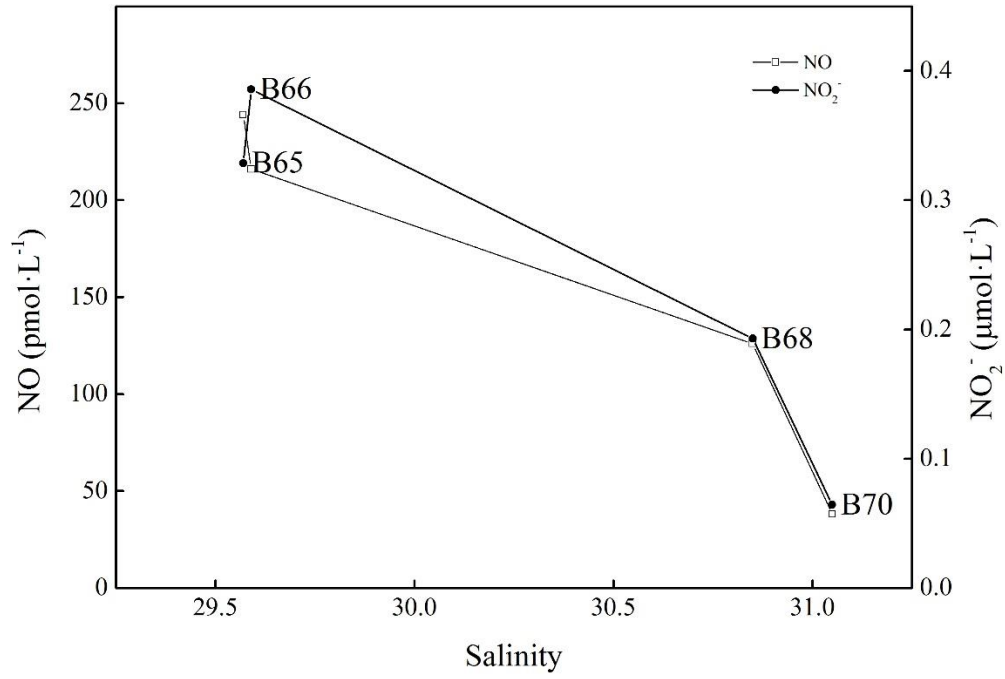

Figure 3. Variations of salinity, NO surface concentrations, and NO_2^- concentrations from station B65 to station B70.

Biogeosciences Discuss., https://doi.org/10.5194/bg-2018-446
Manuscript under review for journal Biogeosciences
Discussion started: 1 November 2018

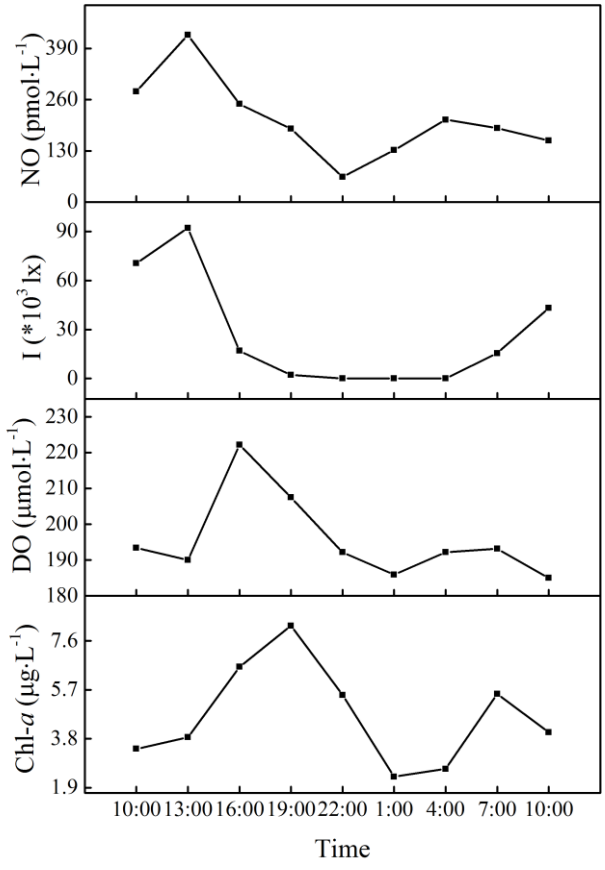

Figure 4. Diurnal variations of NO concentrations, illuminance (I), DO, and Chl-*a* concentrations in the surface water at the anchor station B65.

Biogeosciences Discuss., https://doi.org/10.5194/bg-2018-446
Manuscript under review for journal Biogeosciences
Discussion started: 1 November 2018

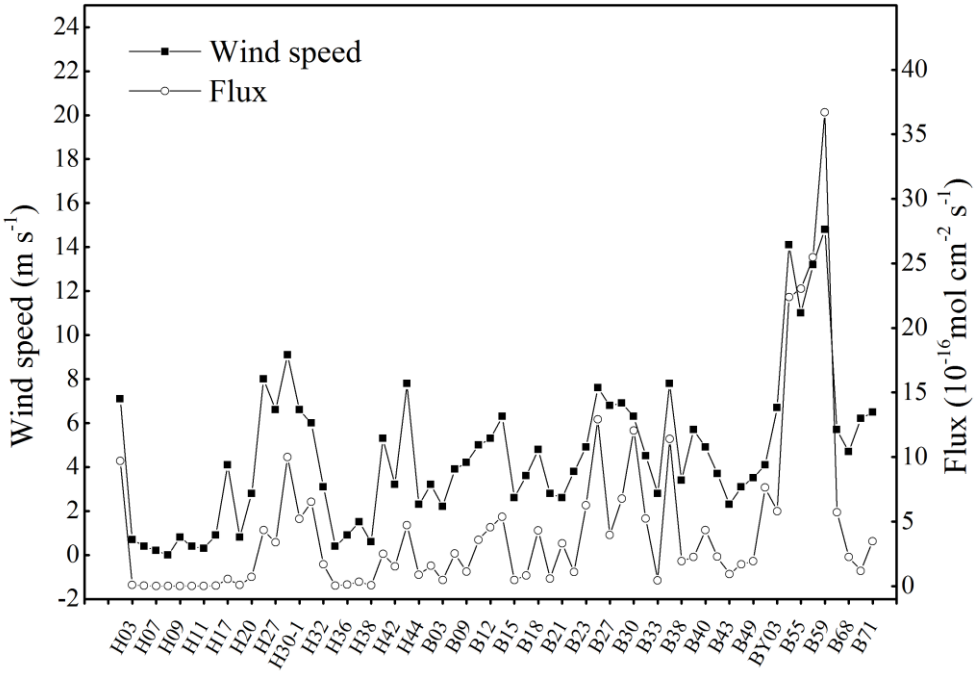

Figure 5. Wind speeds and flux densities of NO from the Bohai and Yellow Seas.

Table Captions

Table 1 Description of sampling stations and seawater temperature (T), salinity (S), Chl-*a* concentrations, DO, illuminance (I), and NO concentrations in the BS and the YS.

Table 2 Description of sampling stations and their seawater temperature, illumination intensity, and photoproduction rates in the BS and the YS.

Table 3 NO Concentrations of different regions in literatures.

Biogeosciences Discuss., https://doi.org/10.5194/bg-2018-446
Manuscript under review for journal Biogeosciences
Discussion started: 1 November 2018

Table 1 Description of sampling stations and seawater temperature (T), salinity(S), Chl-*a* concentrations,

Station	Location	Depth (m)	Local time	T_{surf} (℃)	T_{bott} (℃)	S_{Surf} ‰	S_{bott} ‰	Chl-a_{surf} (μg Ł$^{-1}$)	DO_{surf} (μM)	DO_{bott} (μM)	I (lx)	$[NO]_{surf}$ (pM)	$[NO]_{bott}$ (pM)
H01	121.03 °E, 35.97 °N	33	1928	15.0	9.7	31.72	31.76	0.565	233.35	265.84	169	257	196
H03	121.67 °E, 35.97 °N	37	2250	18.3	8.8	31.73	31.68	0.726	212.8	242.69	32	248	<LOD
H05	122.33 °E, 35.97 °N	55	0238	17.1	6.3	31.50	32.25	0.207	231.82	203.8	32	253	206
H07	123.00 °E, 35.97 °N	71	0618	17.0	7.7	31.55	32.93	0.446	226.54	199.21	19090	195	195
H08	123.50 °E, 35.96 °N	75	0929	17.1	7.7	32.35	32.99	7.674	222.67	194.6	57700	407	295
H09	123.50 °E, 35.50 °N	76	1240	18.3	7.8	32.20	33.05	7.284	215.41	202.61	101500	32	57
H10	123.50 °E, 34.99 °N	77	1546	18.7	7.8	32.53	33.16	3.206	218.32	197.55	13200	110	148
H11	123.00 °E, 35.00 °N	72	1842	19.1	8.1	31.97	33.36	2.587	220.06	196.44	58	90	135
H13	122.34 °E, 35.01 °N	62	2242	19.0	7.7	31.67	32.87	0.521	215.07	199.33	32	<LOD	78
H15	121.65 °E, 35.00 °N	46	0235	19.6	6.3	31.59	32.00	0.627	207.00	213.24	32	35	<LOD
H17	121.00 °E, 35.00 °N	38	0612	18.4	10.5	31.19	31.86	2.400	224.96	229.62	33900	41	81
H19	120.34 °E, 35.00 °N	28	1013	17.2	15.3	31.62	31.71	1.375	220.03	218.6	98700	172	55
H20	120.66 °E, 34.51 °N	20	1354	19.0	18.8	30.01	30.00	0.470	216.86	207.34	77400	113	122
H21	121.00 °E, 34.00 °N	19	1733	20.4	20.1	31.00	30.88	0.597	191.46	194.87	6490	NA	NA
H23	121.66 °E, 34.00 °N	20	2104	19.1	19.1	31.96	31.96	4.417	197.10	196.78	32	NA	244
H25	122.33 °E, 34.00 °N	40	0112	19.3	9.8	32.00	32.51	5.632	211.41	225.14	32	86	78
H27	123.08 °E, 34.00 °N	70	0618	18.9	8.8	32.73	33.36	4.938	205.1	204.93	10122	99	104
H29	124.00 °E, 33.99 °N	82	1257	19.2	9.1	32.63	33.71	13.933	208.46	180.25	65183	153	232
H30-1	124.00 °E, 33.50 °N	69	1615	18.4	10.1	31.79	33.65	1.047	226.07	198.98	12780	153	70
H31	123.99 °E, 32.99 °N	49	1912	18.6	11.9	31.68	32.72	1.593	222.42	191.59	11330	231	<LOD
H32	123.50 °E, 33.00 °N	39	2130	18.4	13.8	31.65	32.27	15.783	229.45	191.93	32	226	NA
H33	122.99 °E, 33.00 °N	36	2352	17.6	14.8	31.91	32.15	7.636	224.52	198.59	32	NA	124
H35	122.35 °E, 33.00 °N	36	0358	17.6	17.6	31.69	31.71	3.195	210.63	211.31	32	233	154
H36	122.00 °E, 33.00 °N	14	0610	18.4	18.4	31.98	31.99	2.272	198.29	197.87	44800	183	102
H37	122.29 °E, 32.31 °N	25	1037	19.1	19.0	30.95	31.08	5.725	181.50	180.75	22200	189	68
H38	122.50 °E, 31.97 °N	27	1328	19.2	18.3	29.65	31.28	6.407	177.64	147.26	9620	179	237
H39	123.02 °E, 31.97 °N	38	1600	18.6	18.5	31.89	31.89	3.406	180.44	178.31	18140	114	36
H41	124.00 °E, 32.00 °N	43	2125	17.2	17.1	31.41	31.45	1.090	202.38	201.91	32	NA	376
H42	124.50 °E, 32.00 °N	43	0030	18.7	15.4	31.90	32.24	0.897	225.02	199.71	32	188	271
HF1	123.32 °E, 34.71 °N	78	1635	20.3	8.2	32.38	33.40	0.671	203.16	191.03	10940	97	92

H44	122.67 °E, 35.50 °N	69	2348	19.7	7.6	31.51	32.91	3.712	222.87	185.19	32	205	NA
B01	123.23 °E, 36.26 °N	75	0328	16.9	7.3	31.56	32.80	0.605	240.44	204.71	528	201	95
B03	122.79 °E, 36.65 °N	25.7	0753	15.4	11.7	31.38	31.48	0.236	258.34	243.82	54200	126	311
B05	122.69 °E, 36.98 °N	41	1136	15.5	11.5	31.59	31.62	1.494	247.11	235.10	100000	NA	<LOD
B07	123.17 °E, 36.98 °N	63	1443	20.5	6.7	31.57	32.23	0.309	222.31	237.81	76500	208	60
B09	123.72 °E, 36.98 °N	76	1811	20.0	6.8	31.92	32.42	0.441	211.24	236.46	2440	79	NA
B10	123.99 °E, 36.98 °N	77	1947	21.0	6.8	31.95	32.42	0.312	204.13	227.81	922	177	48
B12	123.06 °E, 37.89 °N	62	0200	18.8	6.4	31.64	32.14	0.149	217.03	235.66	32	207	49
B13	123.25 °E, 38.13 °N	65	0440	18.9	5.9	31.73	32.09	0.398	212.71	257.77	203	172	191
B14	123.48 °E, 38.43 °N	66	0700	19.2	7.1	31.76	32.15	0.427	218.36	262.51	2500	NA	NA
B15	123.72 °E, 38.74 °N	59	0918	19.4	8.7	31.79	32.11	0.274	216.53	262.56	16640	90	<LOD
B17	124.09 °E, 39.21 °N	41	1300	11.3	10.9	31.62	31.65	0.663	260.47	259.75	12930	89	<LOD
B18	123.64 °E, 39.22 °N	49	1528	19.7	8.7	31.39	31.84	0.600	223.91	256.77	5140	236	276
B19	123.36 °E, 38.74 °N	57	1852	19.7	7.3	31.57	32.13	2.276	216.04	264.95	1010	94	161
B21	123.00 °E, 38.75 °N	54	2052	19.7	5.2	31.29	31.98	0.527	214.72	264.49	32	616	123
B22	122.50 °E, 38.75 °N	55	2348	17.4	3.9	30.81	32.03	1.067	246.19	249.64	32	98	192
B23	122.49 °E, 38.44 °N	55	0210	20.1	4.9	31.66	31.93	0.579	207.68	245.58	32	327	154
B25	122.48 °E, 37.94 °N	49	1616	18.4	5.2	31.17	31.79	0.090	224.02	239.04	8720	286	407
B27	122.47 °E, 37.60 °N	27	1903	18.0	14.1	31.16	31.47	0.369	229.34	188.49	203	110	417
B28	121.99 °E, 37.70 °N	22.8	2143	13.3	9.4	31.47	31.60	2.080	270.02	247.82	32	194	453
B30	122.00 °E, 38.20 °N	56	0147	18.7	3.8	31.18	32.02	1.128	217.62	246.15	32	387	338
B32	122.01 °E, 38.70 °N	53	0550	16.1	4.6	30.61	31.91	4.697	240.34	251.92	25000	339	171
B33	121.43 °E, 38.67 °N	61	0752	18.1	5.6	30.82	31.81	2.737	221.37	252.02	28700	72	NA
B35	121.33 °E, 38.40 °N	50	1052	17.0	6.3	30.81	31.75	4.616	237.4	252.03	30900	244	128
B38	120.74 °E, 38.35 °N	22	1530	15.2	12.1	31.19	31.47	1.945	251.83	255.95	15000	223	315
B39	120.45 °E, 38.34 °N	29	2021	13.8	12.3	31.19	31.30	0.706	241.53	240.32	32	94	363
B40	119.78 °E, 38.33 °N	30	2208	14.4	12.1	30.97	31.28	0.382	254.71	245.62	32	243	241
B42	119.44 °E, 38.33 °N	26.8	0550	19.0	12.6	30.64	31.37	1.151	214.26	216.44	19700	211	157
B43	119.00 °E, 38.32 °N	24	0740	18.8	13.9	30.93	31.32	2.667	226.67	188.85	42400	224	208
B45	118.97 °E, 38.67 °N	20.5	1022	19.4	17.2	31.07	31.22	1.612	236.45	208.28	81900	NA	60
B47	118.97 °E, 38.67N	25	1325	17.4	13.0	31.18	31.47	0.133	251.91	212.27	91900	227	NA
B49	118.97 °E, 39.00 °N	21.4	1610	17.6	16.3	31.31	31.37	0.596	270.9	240.59	29000	204	236
B50	119.71 °E, 39.31 °N	26	2010	20.7	11.8	31.25	31.37	0.135	215.16	212.47	32	565	452

B51	120.07 °E, 39.18 °N	24	2220	19.3	14.8	31.21	31.31	0.625	220.94	213.47	32	NA	307
BY03	120.16 °E, 38.96 °N	21	0008	17.7	17.5	31.15	31.15	0.843	242.26	246.04	32	167	482
B52	120.34 °E, 39.10 °N	22	0201	18.6	17.6	31.23	31.22	1.114	245.12	231.72	32	NA	141
BY04	120.58 °E, 38.84 °N	37	0515	16.8	15.8	31.24	31.27	0.423	218.19	206.65	1463	147	125
B55	120.89 °E, 39.29 °N	33	0929	16.9	13.2	31.16	31.36	0.210	231.28	226.55	39500	248	NA
B56	120.91 °E, 39.55 °N	31.6	1124	17.5	14.0	31.29	31.40	0.967	214.96	191.25	70500	189	204
B59	120.44 °E, 39.48 °N	27	1357	17.4	12.7	31.25	31.41	0.232	215.45	192.18	86200	217	185
B65	119.65 °E, 38.86 °N	16	0957	20.8	NA	29.57	NA	0.323	193.56	NA	31800	244	335
B66	119.32 °E, 37.92 °N	14	1225	21.7	21.6	29.59	30.03	0.493	190.04	174.75	35500	216	244
B68	119.41 °E, 37.73N	16.6	1442	21.5	21.1	30.85	30.86	0.757	195.03	179.67	30000	126	63
B70	120.12 °E, 37.72N	17	1717	20.7	19.1	31.05	31.17	0.988	202.73	187.42	109	38	131
B71	120.22 °E, 38.01N	19.9	1939	17.8	17.2	31.18	31.19	0.344	226.72	212.02	53	106	184

NA: not available
<LOD: below the limit of detection

Biogeosciences Discuss., https://doi.org/10.5194/bg-2018-446
Manuscript under review for journal Biogeosciences
Discussion started: 1 November 2018

Table 2 Description of sampling stations and their seawater temperature, illuminance, and photoproduction rates in the BS and the YS.

	Station	I (lx)	T (℃)	photoproduction rate (10^{-11} mol $L^{-1}s^{-1}$)
SYS	H01	7310	15.0	0.21
	H05	57700	17.1	3.18
	H08	57700	17.1	2.92
	H10	57700	18.7	5.07
	H17	57700	18.4	2.79
	H21	57700	20.4	4.37
	H25	16790	19.3	1.28
	H29	16790	19.2	0.00
	H31	16790	18.6	0.51
	H35	16790	17.6	0.22
	H37	16790	19.1	1.17
	H39	18140	18.6	1.29
	H42	18140	18.7	0.16
	B01	9720	16.9	0.28
	B05	9720	15.5	0.05
	B10	9720	21.0	0.09
	Average	27825	18.2	1.47
NYS	B12	15200	18.8	0.45
	B15	15200	19.4	0.09
	B18	15200	19.7	0.22
	B23	15200	20.1	0.69
	B27	30900	18.0	0.27
	B35	30900	17.0	0.10
	Average	20433	18.3	0.33
BS	B42	30900	19.0	1.54
	B47	14000	17.4	0.88
	B51	14000	19.3	0.32
	B68	30900	21.5	1.50
	Average	22450	19.3	1.14

5

Biogeosciences Discuss., https://doi.org/10.5194/bg-2018-446
Manuscript under review for journal Biogeosciences
Discussion started: 1 November 2018

Table 3 NO concentrations and flux densities from different regions.

Regions	[NO] (pmol L^{-1})	NO fluxes (mol $cm^{-2} s^{-1}$)	Sampling date	Sampling depth	Reference
Jiaozhou Bay	157	7.2×10^{-16}	June, July and August, 2010	Surface water	Tian et al., 2015
Jiaozhou Bay and its adjacent waters	160 ± 130	10.9×10^{-16}	March 8-9, 2011	Surface water	Xue et al., 2012
Central equatorial Pacific	46	$> 2.2\times10^{-16}$	July 14 to August 16, 1978	Surface water	Zafiriou and McFarland, 1981
Eastern tropical North Pacific Ocean	0-65	-	November, 1983	0-3500m	Ward and Zafiriou, 1988
Eastern tropical South Pacific Ocean off Peru	<500-9500	-	February 6 to March 11, 2013	Surface-327 m	Lutterbeck et al., 2018
Coastal water off Qingdao	260 ± 140	-	November, 2009	Surface water	Liu et al.,2017
Seto Inland Sea, Japan	24-320	3.55×10^{-16}	October 5-9, 2009	Surface water	Olasehinde et al, 2010
Yellow Sea and Bohai Sea	Surface: 186 ± 108 Bottom: 174 ± 123	4.5×10^{-16}	June 13-28, 2011	1 m and 1 m above the bottom	This study